

Lipid vesicular gels for topical administration of antioxidants

<https://doi.org/10.1016/j.colsurfb.2022.112388>

Marco Fornasier,^{a,b,\$,} Francesca Dessì,^{a,b,\$} Rosa Pireddu,^c Chiara Sinico,^c Emiliano Carretti,^{b,d} Sergio Murgia^{b,c,*}*

^aDepartment of Chemical and Geological Sciences, University of Cagliari, s.s 554 bivio Sestu, Monserrato I-09042, Italy

^bCSGI, Consorzio Interuniversitario per lo Sviluppo dei Sistemi a Grande Interfase, via della Lastruccia 3 Sesto Fiorentino, Florence, I-50019, Italy

^cDepartment of Life and Environmental Sciences, University of Cagliari, via Ospedale 72, Cagliari I-09124, Italy

^dChemistry Department “Ugo Schiff”, University of Florence and

^{\$} These authors contributed equally to the study.

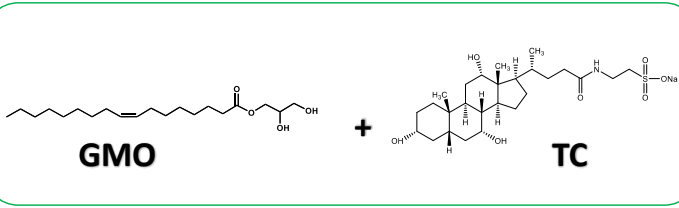
Corresponding authors:

Marco Fornasier (mforneasier@unica.it)

Sergio Murgia (murgias@unica.it)

19 Graphical Abstract

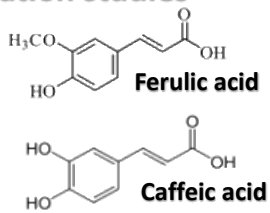
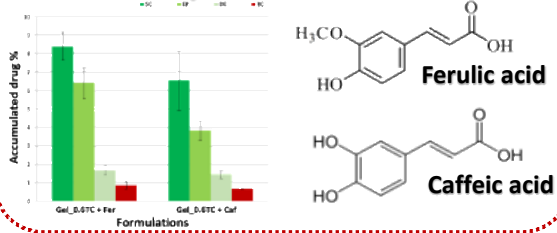
Lipid Vesicular Gels



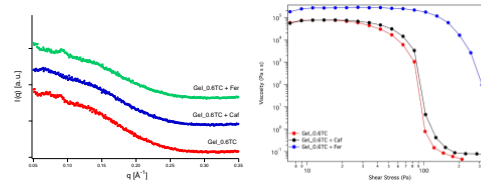
ultrasonication
in water



In vitro permeation studies



Physico-chemical characterization



20

21 **Abstract**

22 The application of a formulation on the skin represents an effective way to deliver bio-active
23 molecules for therapeutical purposes. Moreover, the outermost skin layer, the *stratum corneum*,
24 can be overcome by employing chemical permeation enhancers and edge activators as
25 components. Several lipids can be considered as permeation enhancers, such as the ubiquitous
26 monoolein, one of the most used building blocks for the preparation of lipid liquid crystalline
27 nanoparticles which are applied as drug carriers for nanomedicine applications. Recent papers
28 highlighted how bile salts can affect the phase behavior of monoolein to obtain drug carriers
29 suitable for topical administration, given their role as edge activators into the formulation.

30 Herein, the encapsulation of natural antioxidants (caffeic acid and ferulic acid) into lipid
31 vesicular gels (LVGs) made by monoolein and sodium taurocholate (TC) in water was studied
32 to produce formulations suitable for topical application. TC induce a bicontinuous cubic to
33 multilamellar phase transition for monoolein in water at the given concentrations, and by
34 increasing its content into the formulations, unilamellar LVGs are formed. The encapsulation
35 of the two antioxidants did not affect significantly the structure of the gels. The rheological
36 studies showed that ferulic acid has a structuring effect on the lipid matrix, in comparison with
37 the empty dispersion and the one containing caffeic acid.

38 These gels were then tested *in vitro* on new-born pig skin to evaluate their efficacy as drug
39 carriers for topical administration, showing few differences in the penetration mechanism of
40 the two formulations.

41

42

43

44

45

46 **KEYWORDS**

47 Unilamellar vesicles; monoolein; bile salts; sodium taurocholate; skin.

48 1. Introduction

49 Monoolein is a ubiquitous lipid that is recognized as a safe component in many formulations.
50 Its phase behaviour is characterized by a rich polymorphism. Depending on the water content
51 and the temperature,[1] several liquid crystalline phases can be formed, such as lamellar,
52 inverse hexagonal and inverse bicontinuous cubic phases. An interesting feature of these bulk
53 phases is that they can be dispersed in aqueous solution *via* bottom-up or top-down approaches
54 to obtain lipid liquid crystalline nanoparticles (LLCNPs).[2] They display the same inner
55 structure of the corresponding bulk, but they are much less viscous, an appealing character for
56 biomedical applications. Indeed, LLCNPs such as vesicles,[3–6] hexosomes[7–9] and
57 cubosomes[10–13] have been suggested in nanomedicine as drug and imaging probes carriers.
58 Given the resemblance with cell membranes, the dispersions of the lamellar phase have been
59 widely characterized as drug carriers. Their peculiar architecture allows loading with both
60 hydrophilic and hydrophobic payloads in the aqueous core or in the lipid bilayer, respectively.
61 Several types of vesicles were prepared and tested, using various surfactants to improve their
62 physico-chemical and biological performances for both topical[14] and systemic
63 administrations.[15] In the former case, many papers reported the ability of niosomes,[16,17]
64 ethosomes[18,19] and transferosomes[14,20] to overcome the outermost layer of the skin, the
65 stratum corneum (SC).
66 The dermal/transdermal delivery of a bio-active compound is a non-invasive and safe route,
67 especially in order to avoid the first-pass metabolism.[21] When a molecular dispersion of the
68 drug is applied on the skin, the SC restricts the diffusion of the drug through it. SC is composed
69 by a brick and mortar structure,[22] where the brick is represented by non-living corneocytes
70 immersed in a dense collagen-rich lamellar phase, which represents the mortar. The alternation
71 of hydrophilic and hydrophobic layers hinders the diffusion of molecules, hence affecting the
72 therapeutic outcome. However, this challenging barrier can be overcome by encapsulating the
73 drug within formulations containing permeation enhancers, such as lipids, since they are able
74 to fluidify the lipids in the SC, thus permitting the delivery of the encapsulated payload in the
75 deeper skin *strata*. In addition to permeation enhancers, edge activators can be added to the
76 formulation. They act as softener for lipid bilayers, increasing the elasticity and the
77 deformability of the carrier. Molecules such as bile salts,[9,23] cholesterol[24] and
78 polyethoxylated lipids[25] are recognized as edge activators.
79 Among the different payloads which can be encapsulated, antioxidants have been quite
80 exploited due to their pharmaceutical versatility, working as adjuvants, additives and drugs.
81 Hydroxycinnamic acids such as caffeic (Caf) and ferulic (Fer) acid are secondary metabolites

82 and occur widely in the plant kingdom.[26,27] They exhibit a strong antioxidant activity, that
83 has been tested both *in vitro* and *in vivo*. Caf and its derivatives can directly trap free radicals
84 or scavenge them through several complex reactions. This feature is suitable to formulate gels
85 and cream with anti-photoaging effects. Therefore, Caf and Fer have been encapsulated in
86 several liposomal formulations for topical administration.[28]

87 Due to the beforehand discussed reasons, lipid vesicular gels (LVGs)[29,30] made with a well-
88 known permeation enhancer (MO) and an edge activator (sodium taurocholate, TC) were here
89 prepared in order to deliver caffeic acid and ferulic acid through the skin. This paper covers
90 the physico-chemical characterization of the unloaded and loaded gels (SAXS and Rheology)
91 and the *in vitro* permeation tests on new-born pig skin in order to assess the applicability of
92 these formulations for local administration of antioxidants.

93

94 **2. Material and Methods**

95 **2.1. Chemicals**

96 Monoolein (GMO, glycerol-monooleate, 98.1 %) was kindly provided by Danisco Ingredients
97 (Denmark). Sodium taurocholate (TC, TLC quality, purity ≥ 97.0 %), caffeic acid (HPLC
98 quality, purity ≥ 98.0 %) and ferulic acid (HPLC quality, purity ≥ 98.0 %) were purchased from
99 Sigma-Aldrich.

100 In order to prepare the formulations, ultrapure water was used after filtration through a Milli-
101 Q system (Millipore). The compositions of the samples are given as % w/w.

102

103 **2.2. Lipid Vesicular Gels preparation (LVGs)**

104 LVGs were prepared by dispersing the molten MO in an aqueous solution of TC *via*
105 ultrasonication using a UP100H ultrasonic processor developed by Hiescher for 25 minutes
106 (amplitude of the sonication 90 %, 1 s of pulse ON followed by 1 s of break). Slightly milky
107 or clear gels were obtained depending on the concentration of TC.

108 Samples containing caffeic acid (Caf) and ferulic acid (Fer) were prepared using the same
109 protocol by dispersing the antioxidants into the molten GMO with the help of a vortex until the
110 mixture appeared homogeneous, before adding the aqueous solution of the bile salt. The gels
111 containing Fer and Caf appeared slightly milky and clear, respectively.

112

113 **2.3. Small angle X-ray scattering measurements**

114 The structure of the LVGs was investigated by means of small angle X-ray scattering
115 measurements, using a S3-MICRO SWAXS Camera from HECUS X-ray Systems (Graz,

116 Austria). The X-ray source (GeniX) produced a Cu K α 1.542 Å, working at 30 kV and 0.4 mV.
117 The scattering was detected by a 1D-PSD-50 system from HECUS X-ray Systems (Graz,
118 Austria) containing 1024 channels (width 54.0 μ m). The gels were placed on a stainless steel
119 sample sandwich-type holder, using a polymeric film as windows (Bratfolie, Kalle). The
120 sample-detector distance was kept constant for each experiment (235 mm), giving a working q
121 range $0.003 \leq q \leq 0.6 \text{ \AA}^{-1}$.

122 The scattering patterns of the LVGs were acquired in the temperature range 25 – 50 °C and the
123 temperature was kept constant via a Peltier instrument. The chamber was kept under vacuum
124 during the SAXS experiments to avoid scattering from air. The q scale was calibrated using
125 silver behenate as a standard.

126

127 **2.4. Oscillatory rheology measurements**

128 Oscillatory shear measurements were performed by using a plate-plate geometry (20 mm
129 diameter, 300 μ m gap) with a TA Instruments Discovery Hybrid Rheometer working in
130 controlled shear stress mode. The dependence of the storage modulus (G') and loss modulus
131 (G'') as a function of the angular frequency was investigated in the linear viscoelastic regime
132 of deformations (LVR; strain 0.4 %) in the frequency range $10^{-2} - 10^2$ Hz at a temperature of
133 (25.00 ± 0.01) °C. For each sample investigated, the LVR was determined through a
134 preliminary amplitude sweep experiment (strain range: 0.001-20 %; oscillation frequency: 1
135 Hz).

136 The dependence of G' and G'' on the imposed oscillation frequency was obtained from the
137 phase lag between the applied shear stress and the related flow.

138

139 **2.5. *In vitro* penetration and permeation studies**

140 The ability of LVGs to modulate the antioxidants penetration and/or permeation through the
141 skin was evaluated using skin from new-born pigs. The experiments were performed in Franz
142 vertical cells, exhibiting a diffusion area of 0.785 cm². The skin of one-day-old Goland–
143 Pietrain hybrid pigs (~1.2 kg), died of natural causes and provided by a local slaughterhouse,
144 was excised and stored at –80 °C until the day of the experiment. Skin specimens (n = 6 per
145 formulation) were pre-equilibrated with saline (NaCl 0.9 % w/v) at 25 °C, then sandwiched
146 between the donor and the receptor compartments. The receptor was filled with 5.5 mL of
147 saline solution (NaCl 0.9 w/v %), continuously stirred and thermostated at (37 ± 1) °C, to
148 emulate *in vivo* conditions. 200 mg of each LVG formulations were placed onto the skin

149 surface. At regular intervals, up to 8 h, the receiving solution was entirely withdrawn, replaced
150 with fresh saline to ensure sink conditions and analysed by HPLC for Caf and Fer content.
151 After 8 h, the skin surface was gently washed with 1 mL of distilled water and then dried with
152 filter paper. The stratum corneum was removed by stripping with adhesive tape Tesa® AG
153 (Hamburg, Germany). Each piece of adhesive tape was firmly pressed on the skin surface and
154 rapidly pulled off with one stroke. Epidermis was separated from dermis with a surgical scalpel.
155 Skin *strata* were cut, placed each in a flask with methanol and sonicated for 2 min to extract
156 the accumulated drug. The tape and tissue suspensions were filtered out and assayed for drug
157 content by HPLC.

158

159 **2.6. HPLC quantification of the antioxidants**

160 Caf or Fer content was quantified at 321 nm using a chromatograph Alliance 2690 (Waters,
161 Italy). The column was a XSelect HSS T3 (3.5 μm , 4.6 \times 100 mm, Waters). The mobile phase
162 was a mixture of acetonitrile, water and acetic acid (95.35:4.5:0.15 v/v), delivered at a flow
163 rate of 0.5 mL/min. A standard calibration curve (R^2 of 0.999) was built up by using working,
164 standard solutions (1–100 ng/ μL).

165

166 **2.7. Statistical analysis of data**

167 Results are expressed as the mean \pm standard deviation (SD). Multiple comparisons of means
168 (one-way ANOVA with post-hoc Tukey HSD test) were used to substantiate statistical
169 differences between the datasets, while Student's t-test was used to compare two samples. Data
170 analysis was carried out with the software package XLStatistic for Microsoft Excel.
171 Significance was tested at 0.05 level of probability (p).

172

173

174 **3. Results and Discussion**

175

176 ***SAXS investigations***

177 In order to design a formulation suitable for topical administration of caffeic and ferulic acid,
178 LVGs were obtained by mixing a chemical permeation enhancer (MO) with an aqueous
179 solution of an edge activator (TC). The MO/W phase diagram[1] at high water dilution (higher
180 than 50 % of water, close to room temperature) predicts the existence of a bicontinuous cubic
181 Pn3m phase coexisting with excess of water. However, it was shown that TC affects the MO
182 phase behavior inducing a cubic-to-lamellar phase transition already at very low concentration

183 (0.02 wt % for MO concentration equal to 3.3 wt %), thereby allowing the formation of a
 184 stable unilamellar vesicles dispersion in the presence of Pluronic F108, used as stabilizer.[9]
 185 Indeed, the presence of TC molecules affects (reduces) the effective packing parameter of MO
 186 and, consequently, the interfacial curvature of the system, enabling the formation of vesicles.
 187 Once the *volume* fraction of the dispersed phase overcomes the critical value of 0.494,[30]the
 188 vesicles become so densely packed that they can form very viscous LVGs. Here, with the
 189 addition of a small amount of TC to induce the cubic-to-lamellar phase transition of the
 190 dispersion, and a concentration of MO equal to 14.6 wt %, LVGs were formulated to provide
 191 the system with the necessary higher viscosity suitable for topical administration of natural
 192 antioxidants.

193 The compositions of the different LVGs samples are reported in Table 1.

194

195 **Table 1.** Composition of the LVGs samples expressed as the total amount of lipids and
 196 antioxidants (Antiox) dispersed in water (W).

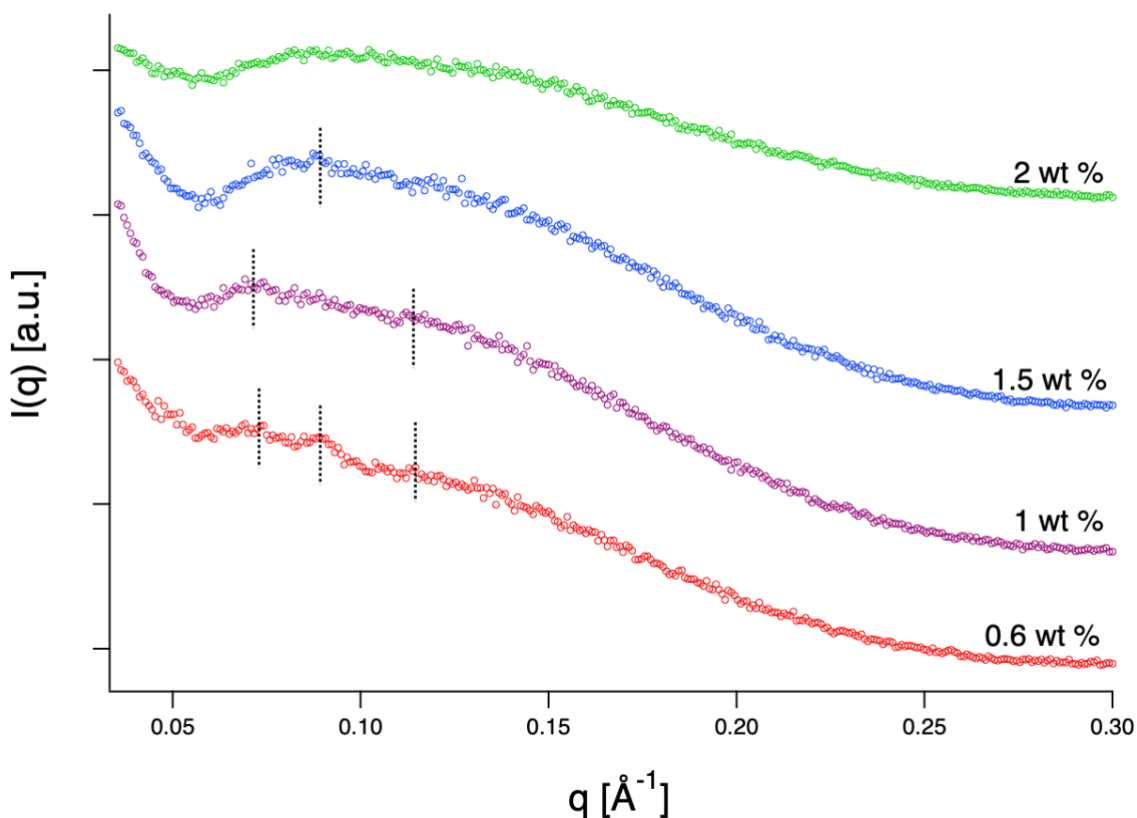
LVGs	MO (wt %)	TC (wt %)	Antiox (wt %)	W (wt%)
Gel_0.6TC	14.6	0.6	-	84.8
Gel_1TC	14.6	1	-	84.4
Gel_1.5TC	14.6	1.5	-	83.9
Gel_2TC	14.6	2	-	83.4
Gel_0.6TC + Caf	14.6	0.6	0.2	84.6
Gel_0.6TC + Fer	14.6	0.6	0.2	84.6

197

198 After visual inspection, the samples appeared stable up to 7-8 weeks at least, without observing
 199 any phase separation. First, the effect of TC on MO/W dispersion was evaluated in the 0.6-2
 200 wt % range of the bile salt.

201 As shown in the Fig. 1, all the samples exhibit a broad diffusive band, as commonly observed
 202 in vesicles dispersions. Depending on the number of double layers characterizing the vesicles,
 203 small quasi-Bragg peaks related to the lamellarity of the system are imposed over the broad
 204 band. The lamellarity, i.e., the number of *lamellae* which divide in sub-compartments the inner
 205 region of the vesicle, represents an important feature to be considered since it is correlated to
 206 the intrinsic stability of the system, to the drug encapsulation efficiency, and to its
 207 release.[3,31]

208



209

210 **Figure 1.** SAXS diffractograms of the LVGs samples at different TC content (wt %) acquired
 211 at 25 °C. The dashed lines highlight the presence of quasi-Brag peaks related to the
 212 multilamellarity of the system.

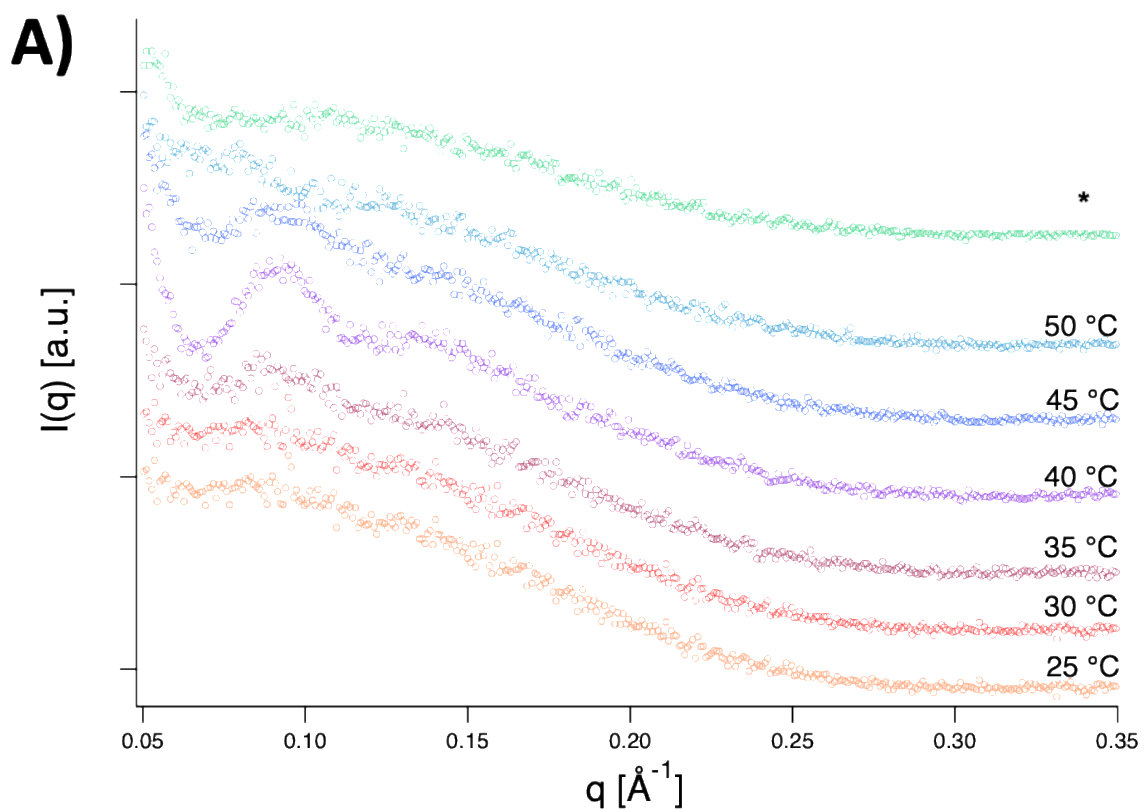
213

214 According to the experimental evidence, showing the disappearance of the quasi-Bragg peaks
 215 related to the Pn3m inverse bicontinuous cubic phase, the lamellarity of the system decreases
 216 by increasing the TC concentration into the formulation, starting from a multilamellar
 217 (Gel_0.6TC) to an unilamellar system (Gel_2TC). The presence of a multilamellar system at
 218 low TC content is not surprising: the MO phase behavior is affected by the presence of the bile
 219 salt, but the BS:MO molar ratio is not enough to give unilamellar vesicles dispersions, as shown
 220 in already reported studies.[9,32] When the BS concentration is increased in the formulation,
 221 the lamellar forming effect leads to a multilamellar-to-unilamellar structural transition, as
 222 already mentioned.

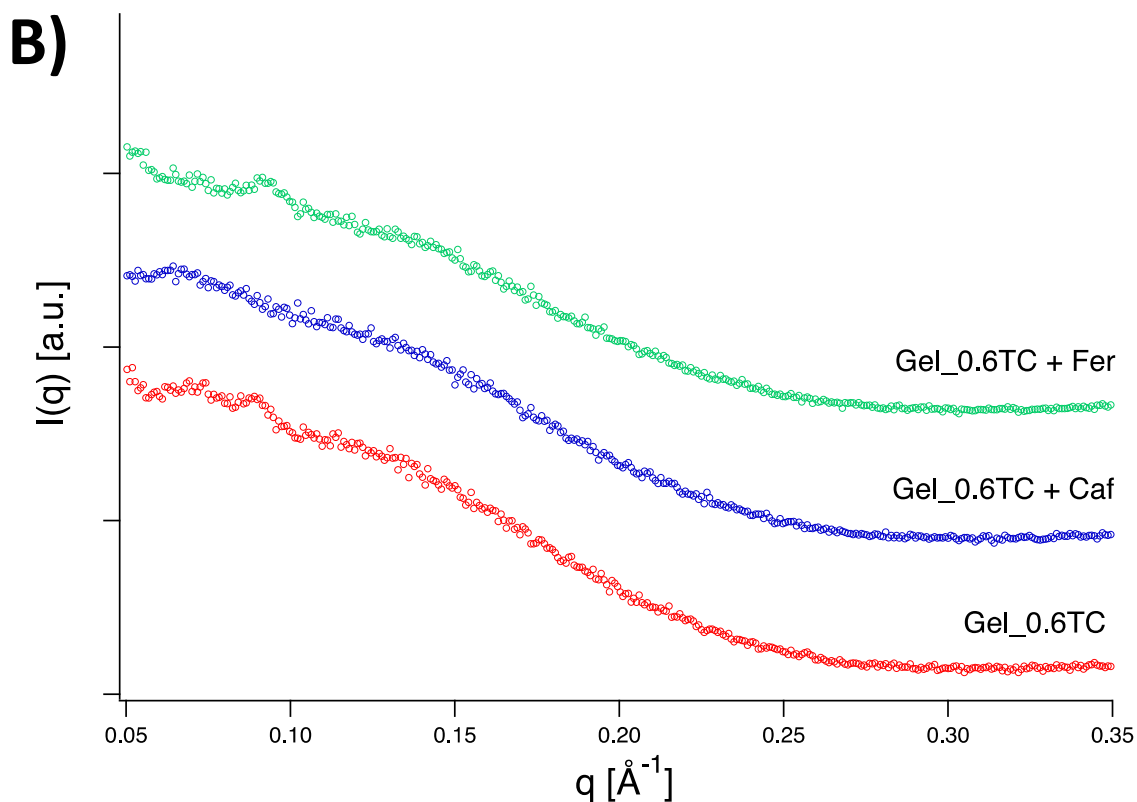
223 Since the temperature of the skin varies depending on the body districts, it can play a role on
 224 its physico-chemical properties, and on the efficacy of the treatment. Therefore, the thermo-
 225 responsive behavior of the Gel_0.6TC was investigated in the range 25-50 °C. Fig. 2A shows
 226 that the quasi-Bragg peaks are more pronounced in the temperature range 35-40 °C.
 227 Apparently, above 40 °C the lamellarity of the system decreases, possibly due to a lower bilayer

228 rigidity that, in turn, favors the unilamellar arrangement. No hysteresis was observed when the
229 sample was cooled down again to 25 °C. The almost perfect overlap between the two scattering
230 curves (before and after the heating cycle) represents a sign of a reversible physical
231 transformation into the formulation.

232



233



234

235

236 **Figure 2.** A) Thermo-responsive behavior of the LVG Gel_0.6TC in the range 25-50 °C and
 237 then back to 25 °C (described by the presence of *). B) Effect of the encapsulation of the
 238 antioxidants on the SAXS profile of the LVG Gel_0.6TC at 25 °C.

239

240 Considering these features, the sample Gel_0.6TC was loaded with the natural antioxidants
 241 caffeic acid (Caf) and ferulic acid (Fer) at a concentration of 2 mg g⁻¹.

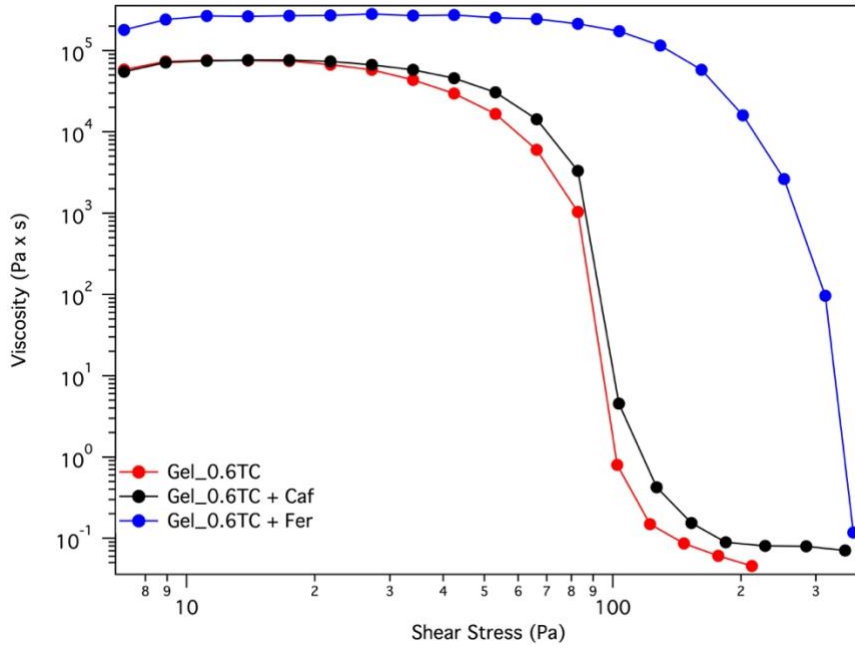
242 The gel loaded with Fer appeared slightly milkier than the unloaded LVG, whereas the one
 243 containing Caf was yellowish. The SAXS patterns of these samples are reported in Fig. 2B,
 244 using the empty formulation as a reference. In general, this comparison proved that the
 245 presence of these two additives did not affect significantly the gel structure.

246

247 ***Rheological features of the LVGs***

248 Given the macroscopical gel appearance, samples were characterized by means of rheology.
 249 The flow curves of the samples Gel_0.6TC, Gel_0.6TC + Caf and Gel_0.6TC + Fer are
 250 reported in Fig. 3.

251



252

253

254 **Figure 3.** Flow curves of the empty Gel_0.6TC (red), Gel_0.6TC + Caf (black) and Gel_0.6TC
 255 + Fer (blue).

256

257 All the investigated samples are characterized by a Newtonian behavior in the low shear stress
 258 regime while for higher perturbations they exhibit a shear-thinning behavior as indicated by
 259 rapid decrease of the viscosity occurring at high shear stress. As indicated in Figure 4,
 260 Gel_0.6TC and Gel_0.6TC + Caf exhibit almost the same viscosity value in the whole
 261 investigated shear stress range indicating that the loading of caffeic acid does not affect
 262 meaningfully the structure of the gel system. Nevertheless, Gel_0.6TC + Fer sample has a
 263 higher viscosity over the whole investigated shear stress range; this effect could be ascribed to
 264 the structuring effect played by the ferulic acid into the gel matrix, which induces a harder and
 265 more compact structure to the LVG in comparison to the empty gel.

266 The flow curves were fitted using the Cross model (equation 1.):

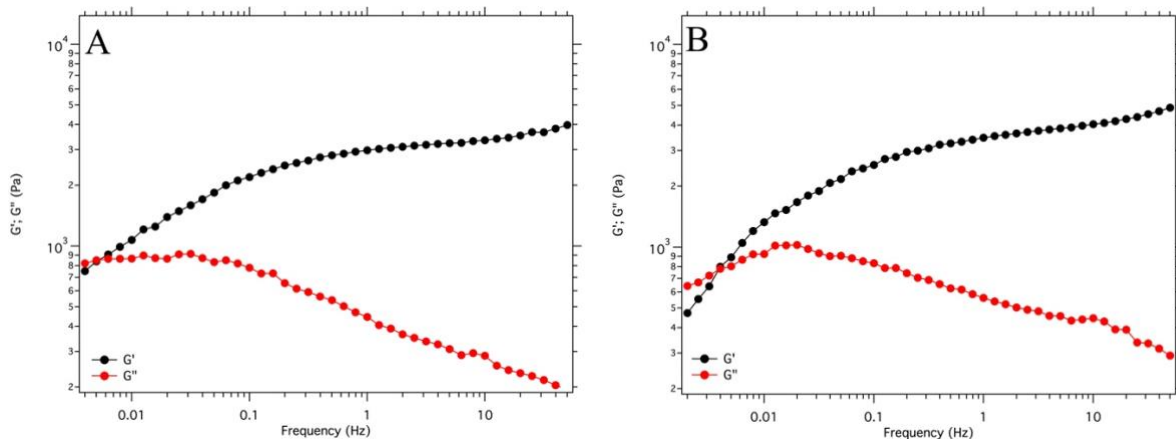
267

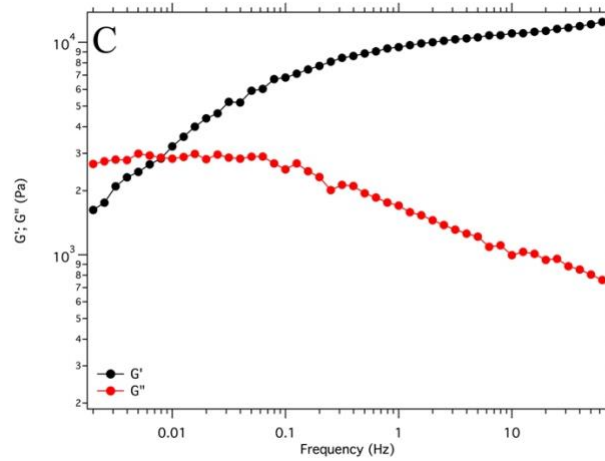
$$268 \quad \eta = \eta_{\infty} + \frac{(\eta_0 - \eta_{\infty})}{1 + (C\dot{\gamma})^m} \quad Eq. 1$$

269

270 where η_{∞} is the viscosity at plateau for high shear stress (in the studied case $\eta_{\infty}=0$ since the
 271 curves did not reach a plateau at high shear stress values); η_0 is the viscosity at low shear rate
 272 at the plateau and it represents an intrinsic viscosity of the fluid; m is the Cross rate constant

273 that yields the velocity gradient dependence of the rate in the shear thinning region; C is the
 274 Cross time constant (called also consistency of the material) that has the dimensions of time.
 275 $1/C$ indicates a critical shear rate that corresponds to the onset shear rate for shear thinning.
 276 In Fig. S11, the fittings of the flow curves are shown; the outputs data obtained from the fitting
 277 are listed in Tab S11. The data listed in Table S11 clearly indicate that the encapsulation of
 278 caffeic acid did not affect in a significant way the rheological features of the system Gel_0.6TC
 279 since the pure and the doped gel show almost identical parameters. On the other hand, the
 280 formulation containing ferulic acid exhibits a higher η_0 , highlighting the structuring effect of
 281 the antioxidant into the LVG. The values of the Cross-rate constant are similar for all the
 282 samples, indicating a similar shear rate-dependence of the viscosity in the shear thinning
 283 region.
 284 Furthermore, the viscoelastic properties of the LVGs before and after the loading caffeic acid
 285 and ferulic acid, were studied via oscillatory rheology by means of frequency sweep
 286 experiments. All the measurements were carried out into the LVR previously identified through
 287 amplitude sweep tests (see Figure S11). In all the frequency sweep experiments, the strain value
 288 was fixed to 0.05 % (Fig. 4).
 289





290 **Figure 4.** Frequency sweep curves for Gel_0.6TC (A), Gel_0.6TC + Caf (B) and Gel_0.6TC
 291 + Fer (C).

292

293 Figure 4 shows that all the samples have a similar behavior, typical of viscoelastic fluids. At
 294 high oscillatory frequencies, the elastic contribution prevails since $G' > G''$ while below the
 295 crossover frequencies, the samples exhibit a viscous behavior ($G'' > G'$). Gel_0.6TC + Fer is
 296 characterized by an asymptotic value of G' at high frequency, that corresponds to the intrinsic
 297 elastic modulus of the system, that is almost five times higher than the two other gels. This
 298 finding confirms the structuring effect that Fer has on the Gel_0.6TC system.

299 Since the dynamic of the investigated gels cannot be described by a single element Maxwell
 300 model, the best approach to study the typical relaxation time of the investigated gels is to
 301 consider the relaxation time spectrum $H(\tau)$ that depends upon G' and G'' as indicated by the
 302 following equations 2 and 3:

303

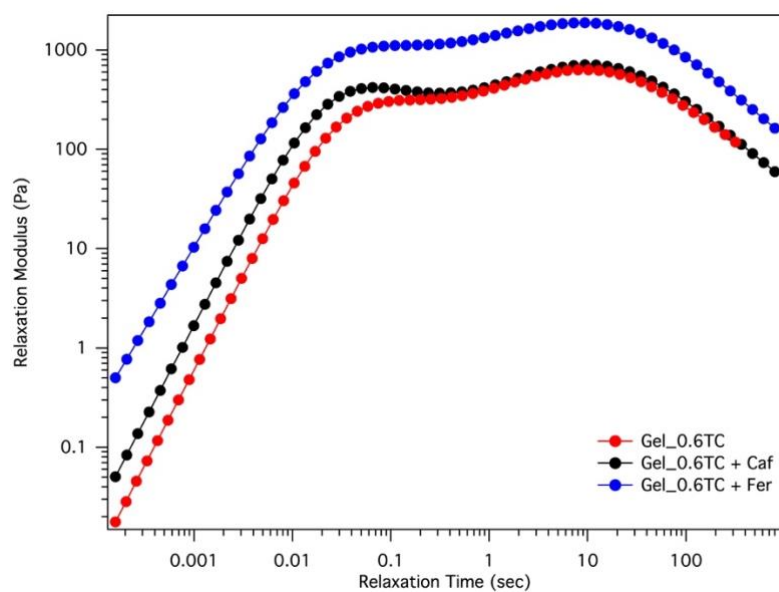
$$304 \quad G'(\omega) = G_0 + \int_0^{\infty} H(\tau) \frac{(\omega\tau)^2}{1 + (\omega\tau)^2} \frac{d\tau}{\tau} \quad Eq. 2$$

$$305 \quad G''(\omega) = G_0 + \int_0^{\infty} H(\tau) \frac{\omega\tau}{1 + (\omega\tau)^2} \frac{d\tau}{\tau} \quad Eq. 3$$

306

307 Where $H(\tau)$ can be obtained following different algorithms for the inversion of the equation
 308 (1) and (2).[33]

309



310
311
312
313
314

Figure 5. Relaxation plots of the Gel_0.6TC (red), Gel_0.6TC + Caf (black) and Gel_0.6TC + Fer (blue).

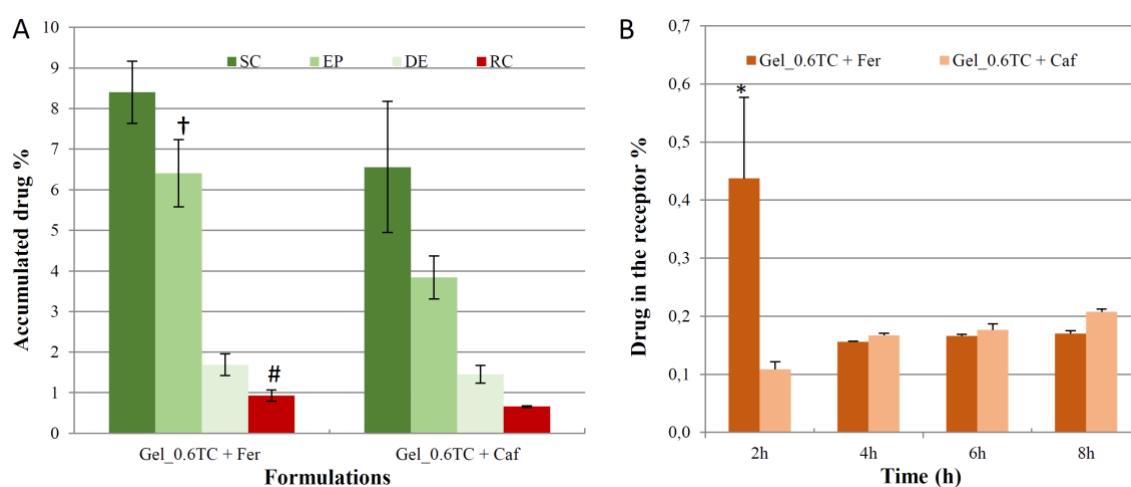
315 The relaxation mechanical spectra of the investigated LVGs are reported in Figure 5 and
316 provide information about the distribution of the relaxation times; the profile of the curves is
317 similar and indicates that the encapsulation of the two antioxidants in the lipid matrix do not
318 affect the relaxation mechanism that remains almost unchanged, as indicated by the persistence
319 of the position of the peaks. Nevertheless, the loading of ferulic acid slightly rises the relaxation
320 modulus, confirming again the structuring character of this additive and the higher compactness
321 of the Gel_0.6TC+Fer.

322

323 *In vitro penetration studies on skin*

324 Caf and Fer delivery into and through new-born pig skin was evaluated *in vitro* under non-
325 occlusive conditions, using vertical Franz diffusion cells. These investigations showed the
326 ability of the LVGs to facilitate the accumulation of both antioxidants within the different skin
327 strata. As shown in Fig. 6A, the accumulation profile of the two molecules in the three layers
328 is very similar: the largest amount of the drug was found in the outermost layers of the skin,
329 stratum corneum (SC, 8.40% for Gel_0.6TC + Fer and 6.55% for Gel_0.6TC + Caf) and
330 epidermis (EP, 6.40% for Gel_0.6TC + Fer and 3.83% for Gel_0.6TC + Caf) while
331 significantly lower concentrations were found in the dermis (D, 1.69% for Gel_0.6TC + Fer
332 and 1.45% for Gel_0.6TC+ Caf) and in the receptor compartment (0.93% for Gel_0.6TC + Fer
333 and 0.66% for Gel_0.6TC + Caf) after 8 hours of treatment.

334 Nevertheless, some differences emerged by comparing the two antioxidants' profiles: the
 335 amount of Fer found in the uppermost layers of the skin (SC + EP) is greater than that of caffeic
 336 acid accumulated in the same layers (about 15 % Gel_0.6TC + Fer and about 10% Gel_0.6TC
 337 + Caf), and we found about 67 % more ferulic acid in the epidermis than caffeic acid. Moreover,
 338 as can be observed in Figure 6A, after just two hours of treatment, ferulic acid is found three-
 339 fold higher than caffeic acid in the receptor compartment. As well known, the absorption of
 340 molecules through the skin is affected by physicochemical features of the molecule itself, and
 341 its *logP* value can provide useful information and predict the behavior. Our results are perfectly
 342 in accordance with what was previously reported in the literature. Particularly, Saija *et al* tested
 343 percutaneous diffusion of Fer and Caf in saturated aqueous solutions and explained the higher
 344 skin absorption of Fer due to its higher lipophilicity, with respect to caffeic acid.[34,35]
 345 Moreover, Matri-Mestres *et al.* found limited percutaneous penetration of Caf, even when
 346 applied on the skin with penetration enhancers such as a mixture of transcitol and propylene
 347 glycol.[36]
 348



349
 350
 351 **Figure 6.** A) Amount of Fer and Caf retained into and permeated through the skin layers after
 352 8 h treatment with Gel_0.6TC + Fer and Gel_0.6TC + Caf. SC, stratum corneum; EP,
 353 epidermis; D, dermis; and RC, receptor compartment. B) Amount of Fer and Caf detected in
 354 the receptor compartment at different time points after the application of Gel_0.6TC + Fer and
 355 Gel_0.6TC + Caf. The amount is expressed as the percentage of the dose applied on the skin.
 356 Results are reported as means \pm standard deviations of at least 6 independent determinations.
 357 Symbols represent significance of differences between Fer and Caf in EP, † $P < 0.05$, between
 358 Fer and Caf in RC, # $P < 0.05$, and between Fer and Caf in RC after 2h, * $P < 0.05$.

359 In conclusion, Caf is mostly retained in the gel and then released more slowly once applied to
360 the skin. Conversely, given its higher lipophilicity [34,35,37], and thanks to the presence of the
361 permeation enhancers TC and MO, Fer is able to permeate all layers and reach the receptor
362 compartment faster than Caf. However, the differences between Fer and Caf loaded LVGs that
363 emerged from the rheological and SAXS studies suggest a different interaction between the
364 antioxidants and the gel matrix, which can subsequently affect the release and
365 accumulation/permeation of the investigated active compounds in/through the skin.

366

367 **4. Conclusion**

368 The application of a formulation on the skin represents an easy and non-invasive way to
369 administrate drugs. In this way, the harsh gastrointestinal environment, which can affect the
370 biodistribution and stability of the formulation, can be bypassed. The *stratum corneum* is
371 indeed a challenging obstacle but the inclusion of permeation enhancers and edge activators in
372 the carriers can improve the effectiveness and the quality of the therapy.

373 Therefore, LVGs were formulated with monoolein and sodium taurocholate to deliver caffeic
374 and ferulic acid. The SAXS investigations highlighted that the presence of TC induces a phase
375 transition from inverse bicontinuous cubic Pn3m, the native structure of GMO at these
376 concentrations, to multilamellar vesicles dispersions. The increasing concentration of TC
377 decreases the lamellarity of the vesicles, whereas the number of lamellae increases in the range
378 35 – 40 °C for the sample at 0.6 % wt of TC. The encapsulation of the antioxidants did not
379 affect the inner structure of LVG at low TC content (0.6 wt %). The LVGs unloaded and loaded
380 with Caf and Fer were studied by means of oscillatory measurements, displaying the shear-
381 thinning behaviour of the formulations and the structuring effect of Fer on the lipid matrix in
382 comparison with the empty LVG and the one loaded with Caf. The skin permeation tests
383 showed the dermal release of both antioxidants, highlighting the applicability of these
384 formulations for topical administration.

385 These findings exhibited the effect of LVGs composed with MO and TC, recognized as safe
386 and used in the cosmetical and pharmaceuticals industries, for local application of bio-actives.
387 Indeed, the interactions of these components with keratinocytes could be evaluated to
388 understand the nature of the permeation phenomena. Some studies showed the applicability of
389 NMR spectroscopy both in solid and liquid state for this purpose.[38] Moreover, formulating
390 a mechanism of penetration of these carriers could represent a future project so to improve and
391 enhance the experimental design for future applications.

392

393 **Acknowledgements**

394 Monica Demurtas and Prof. Flaminia Cesare Marincola are kindly thanked for providing the
395 antioxidants. MF gratefully acknowledges Sardinian Regional Government for the financial
396 support of his Ph.D. scholarship (P.O.R. Sardegna F.S.E. - Operational Programme of the
397 Autonomous Region of Sardinia, European Social Fund 2014-2020 - Axis III Education and
398 training, Thematic goal 10, Investment Priority 10ii, Specific goal 10.5). SM thanks
399 Fondazione Banco di Sardegna and Regione Autonoma della Sardegna (Progetti Biennali di
400 Ateneo Annualità 2018).

401

402

403

404 **References**

- 405 [1] H. Qiu, M. Caffrey, The phase diagram of the monoolein/water system: Metastability
406 and equilibrium aspects, *Biomaterials*. 21 (2000) 223–234.
407 [https://doi.org/10.1016/S0142-9612\(99\)00126-X](https://doi.org/10.1016/S0142-9612(99)00126-X).
- 408 [2] S. Murgia, S. Biffi, R. Mezzenga, Recent advances of non-lamellar lyotropic liquid
409 crystalline nanoparticles in nanomedicine, *Curr. Opin. Colloid Interface Sci.* 48 (2020)
410 28–39. <https://doi.org/10.1016/j.cocis.2020.03.006>.
- 411 [3] M. Schlich, M. Fornasier, M. Nieddu, C. Sinico, S. Murgia, A. Rescigno, 3-
412 Hydroxycoumarin Loaded Vesicles for Recombinant Human Tyrosinase Inhibition in
413 Topical Applications, *Colloids Surfaces B Biointerfaces*. 171 (2018) 675–681.
414 <https://doi.org/10.1016/j.colsurfb.2018.08.008>.
- 415 [4] M. Fornasier, A. Porcheddu, A. Casu, S.R. Raghavan, P. Jönsson, K. Schillén, S.
416 Murgia, Surface-modified nanoerythroosomes for potential optical imaging diagnostics,
417 *J. Colloid Interface Sci.* (2021). <https://doi.org/10.1016/j.jcis.2020.08.032>.
- 418 [5] M. Schlich, C. Sinico, D. Valenti, A. Gulati, M.D. Joshi, V. Meli, S. Murgia, T.
419 Xanthos, Towards long-acting adrenaline for cardiopulmonary resuscitation:
420 Production and characterization of a liposomal formulation, *Int. J. Pharm.* 557 (2019)
421 105–111. <https://doi.org/10.1016/j.ijpharm.2018.12.044>.
- 422 [6] M. Mamusa, F. Barbero, C. Montis, L. Cutillo, A. Gonzalez-Paredes, D. Berti,
423 Inclusion of oligonucleotide antimicrobials in biocompatible cationic liposomes: A
424 structural study, *J. Colloid Interface Sci.* 508 (2017) 476–487.
425 <https://doi.org/10.1016/j.jcis.2017.08.080>.
- 426 [7] V.K. Rapalli, T. Waghule, N. Hans, A. Mahmood, S. Gorantla, S.K. Dubey, G.

- 427 Singhvi, Insights of lyotropic liquid crystals in topical drug delivery for targeting
428 various skin disorders, *J. Mol. Liq.* 315 (2020).
429 <https://doi.org/10.1016/j.molliq.2020.113771>.
- 430 [8] T. Madheswaran, M. Kandasamy, R.J. Bose, V. Karuppagounder, Current potential
431 and challenges in the advances of liquid crystalline nanoparticles as drug delivery
432 systems, *Drug Discov. Today.* 24 (2019) 1405–1412.
433 <https://doi.org/10.1016/j.drudis.2019.05.004>.
- 434 [9] M. Fornasier, R. Pireddu, A. Del Giudice, C. Sinico, T. Nylander, K. Schillén, L.
435 Galantini, S. Murgia, Tuning lipid structure by bile salts: Hexosomes for topical
436 administration of catechin, *Colloids Surfaces B Biointerfaces.* 199 (2021) 1–9.
437 <https://doi.org/10.1016/j.colsurfb.2021.111564>.
- 438 [10] S. Jenni, G. Picci, M. Fornasier, M. Mamusa, J. Schmidt, Y. Talmon, A. Sour, V.
439 Heitz, S. Murgia, C. Caltagirone, Multifunctional cubic liquid crystalline nanoparticles
440 for chemo- And photodynamic synergistic cancer therapy, *Photochem. Photobiol. Sci.*
441 (2020). <https://doi.org/10.1039/c9pp00449a>.
- 442 [11] M. Fornasier, S. Biffi, B. Bortot, P. Macor, A. Manhart, F.R. Wurm, S. Murgia,
443 Cubosomes stabilized by a polyphosphoester-analog of Pluronic F127 with reduced
444 cytotoxicity, *J. Colloid Interface Sci.* 580 (2020) 286–297.
445 <https://doi.org/10.1016/j.jcis.2020.07.038>.
- 446 [12] U. Bazylińska, J. Kulbacka, J. Schmidt, Y. Talmon, S. Murgia, Polymer-free
447 cubosomes for simultaneous bioimaging and photodynamic action of photosensitizers
448 in melanoma skin cancer cells, *J. Colloid Interface Sci.* 522 (2018) 163–173.
449 <https://doi.org/10.1016/j.jcis.2018.03.063>.
- 450 [13] C. Montis, B. Castroflorio, M. Mendozza, A. Salvatore, D. Berti, P. Baglioni,
451 Magnetocubosomes for the delivery and controlled release of therapeutics, *J. Colloid*
452 *Interface Sci.* 449 (2015) 317–326. <https://doi.org/10.1016/j.jcis.2014.11.056>.
- 453 [14] F. Lai, C. Caddeo, M.L. Manca, M. Manconi, C. Sinico, A.M. Fadda, What’s new in
454 the field of phospholipid vesicular nanocarriers for skin drug delivery, *Int. J. Pharm.*
455 583 (2020). <https://doi.org/10.1016/j.ijpharm.2020.119398>.
- 456 [15] M.J. Haney, N.L. Klyachko, Y. Zhao, R. Gupta, E.G. Plotnikova, Z. He, T. Patel, A.
457 Piroyan, M. Sokolsky, A. V. Kabanov, E. V. Batrakova, Exosomes as drug delivery
458 vehicles for Parkinson’s disease therapy, *J. Control. Release.* 207 (2015) 18–30.
459 <https://doi.org/10.1016/j.jconrel.2015.03.033>.
- 460 [16] G. Cevc, Transfersomes, liposomes and other lipid suspensions on the skin:

- 461 Permeation enhancement, vesicle penetration, and transdermal drug delivery, *Crit.*
462 *Rev. Ther. Drug Carrier Syst.* (1996).
463 <https://doi.org/10.1615/CritRevTherDrugCarrierSyst.v13.i3-4.30>.
- 464 [17] S.R.M. Moghddam, A. Ahad, M. Aqil, S.S. Imam, Y. Sultana, Formulation and
465 optimization of niosomes for topical diacerein delivery using 3-factor, 3-level Box-
466 Behnken design for the management of psoriasis, *Mater. Sci. Eng. C.* 69 (2016) 789–
467 797. <https://doi.org/10.1016/j.msec.2016.07.043>.
- 468 [18] A. Mistry, P. Ravikumar, Development and evaluation of azelaic acid based ethosomes
469 for topical delivery for the treatment of acne, *Indian J. Pharm. Educ. Res.* 50 (2016)
470 S232–S243. <https://doi.org/10.5530/ijper.50.3.34>.
- 471 [19] G. Sharma, H. Goyal, K. Thakur, K. Raza, O.P. Katare, Novel elastic membrane
472 vesicles (EMVs) and ethosomes-mediated effective topical delivery of aceclofenac: a
473 new therapeutic approach for pain and inflammation, *Drug Deliv.* 23 (2016) 3135–
474 3145. <https://doi.org/10.3109/10717544.2016.1155244>.
- 475 [20] G. Cevc, Lipid vesicles and other colloids as drug carriers on the skin, *Adv. Drug*
476 *Deliv. Rev.* (2004). <https://doi.org/10.1016/j.addr.2003.10.028>.
- 477 [21] M.R. Prausnitz, R. Langer, Transdermal drug delivery, *Nat. Biotechnol.* 26 (2008)
478 1261–1268. <https://doi.org/10.1038/nbt.1504>.
- 479 [22] P.M. Elias, Structure and function of the stratum corneum extracellular matrix, *J.*
480 *Invest. Dermatol.* 132 (2012) 2131–2133. <https://doi.org/10.1038/jid.2012.246>.
- 481 [23] E. Moghimipour, A. Ameri, S. Handali, Absorption-Enhancing Effects of Bile Salts,
482 *Molecules.* 20 (2015) 14451–14473. <https://doi.org/10.3390/molecules200814451>.
- 483 [24] G.M.M. El Maghraby, A.C. Williams, B.W. Barry, Interactions of surfactants (edge
484 activators) and skin penetration enhancers with liposomes, *Int. J. Pharm.* 276 (2004)
485 143–161. <https://doi.org/10.1016/j.ijpharm.2004.02.024>.
- 486 [25] G.M. El Zaafarany, G.A.S. Awad, S.M. Holayel, N.D. Mortada, Role of edge
487 activators and surface charge in developing ultradeformable vesicles with enhanced
488 skin delivery, *Int. J. Pharm.* 397 (2010) 164–172.
489 <https://doi.org/10.1016/j.ijpharm.2010.06.034>.
- 490 [26] J.H. Chen, C.T. Ho, Antioxidant Activities of Caffeic Acid and Its Related
491 Hydroxycinnamic Acid Compounds, *J. Agric. Food Chem.* 45 (1997) 2374–2378.
492 <https://doi.org/10.1021/jf970055t>.
- 493 [27] I. Gülçin, Antioxidant activity of caffeic acid (3,4-dihydroxycinnamic acid),
494 *Toxicology.* 217 (2006) 213–220. <https://doi.org/10.1016/j.tox.2005.09.011>.

- 495 [28] N.P. Katuwavila, A.D.L.C. Perera, V. Karunaratne, G.A.J. Amaratunga, D.N.
496 Karunaratne, Improved delivery of caffeic acid through liposomal encapsulation, *J.*
497 *Nanomater.* 2016 (2016). <https://doi.org/10.1155/2016/9701870>.
- 498 [29] R. Angelico, M. Carboni, S. Lampis, J. Schmidt, Y. Talmon, M. Monduzzi, S. Murgia,
499 Physicochemical and rheological properties of a novel monoolein-based vesicle gel,
500 *Soft Matter.* 9 (2013) 921–928. <https://doi.org/10.1039/c2sm27215f>.
- 501 [30] M. Gradzielski, Vesicles and vesicle gels - Structure and dynamics of formation, *J.*
502 *Phys. Condens. Matter.* 15 (2003). <https://doi.org/10.1088/0953-8984/15/19/202>.
- 503 [31] M. Fröhlich, V. Brecht, R. Peschka-Süss, Parameters influencing the determination of
504 liposome lamellarity by 31P-NMR, *Chem. Phys. Lipids.* 109 (2001) 103–112.
505 [https://doi.org/10.1016/S0009-3084\(00\)00220-6](https://doi.org/10.1016/S0009-3084(00)00220-6).
- 506 [32] A. Sadeghpour, M. Rappolt, S. Misra, C. V. Kulkarni, Bile Salts Caught in the Act:
507 From Emulsification to Nanostructural Reorganization of Lipid Self-Assemblies,
508 *Langmuir.* 34 (2018) 13626–13637. <https://doi.org/10.1021/acs.langmuir.8b02343>.
- 509 [33] E. Carretti, C. Matarrese, E. Fratini, P. Baglioni, L. Dei, Physicochemical
510 characterization of partially hydrolyzed poly(vinyl acetate)-borate aqueous dispersions,
511 *Soft Matter.* 10 (2014) 4443–4450. <https://doi.org/10.1039/c4sm00355a>.
- 512 [34] A. Saija, A. Tomaino, D. Trombetta, A. De Pasquale, N. Uccella, T. Barbuzzi, D.
513 Paolino, F. Bonina, In vitro and in vivo evaluation of caffeic and ferulic acids as
514 topical photoprotective agents, *Int. J. Pharm.* 199 (2000) 39–47.
515 [https://doi.org/10.1016/S0378-5173\(00\)00358-6](https://doi.org/10.1016/S0378-5173(00)00358-6).
- 516 [35] A. Saija, A. Tomaino, R. Lo Cascio, D. Trombetta, A. Proteggente, A. De Pasquale, N.
517 Uccella, F. Bonina, Ferulic and caffeic acids as potential protective agents against
518 photooxidative skin damage, *J. Sci. Food Agric.* 79 (1999) 476–480.
519 [https://doi.org/10.1002/\(SICI\)1097-0010\(19990301\)79:3<476::AID-](https://doi.org/10.1002/(SICI)1097-0010(19990301)79:3<476::AID-JSFA270>3.0.CO;2-L)
520 [JSFA270>3.0.CO;2-L](https://doi.org/10.1002/(SICI)1097-0010(19990301)79:3<476::AID-JSFA270>3.0.CO;2-L).
- 521 [36] G. Marti-Mestres, J.P. Mestres, J. Bres, S. Martin, J. Ramos, L. Vian, The “in vitro”
522 percutaneous penetration of three antioxidant compounds, *Int. J. Pharm.* 331 (2007)
523 139–144. <https://doi.org/10.1016/j.ijpharm.2006.09.020>.
- 524 [37] F.M.F. Roleira, C. Siquet, E. Orr, E.M. Garrido, J. Garrido, N. Milhazes, G. Podda, F.
525 Paiva-Martins, S. Reis, R.A. Carvalho, E.J.T. Da Silva, F. Borges, Lipophilic phenolic
526 antioxidants: Correlation between antioxidant profile, partition coefficients and redox
527 properties, *Bioorganic Med. Chem.* 18 (2010) 5816–5825.
528 <https://doi.org/10.1016/j.bmc.2010.06.090>.

529 [38] Q.D. Pham, S. Björklund, J. Engblom, D. Topgaard, E. Sparr, Chemical penetration
530 enhancers in stratum corneum - Relation between molecular effects and barrier
531 function, *J. Control. Release.* 232 (2016) 175–187.
532 <https://doi.org/10.1016/j.jconrel.2016.04.030>.
533